

Evaluation of Piezoelectric-based Composite for Actuator Application via FEM with Thermal Analogy

KEVIN, Alexander, AKBAR, Mahesa, GUNAWAN, Leonardo, AULIA, Darryl Khalid, AGUNG, Rizqy, RAWIKARA, Seno Sahisnu, SASONGKO, Rianto Adhy and WIDAGDO, Djarot

Available from Sheffield Hallam University Research Archive (SHURA) at:

<https://shura.shu.ac.uk/34051/>

This document is the author deposited version. You are advised to consult the publisher's version if you wish to cite from it.

Published version

KEVIN, Alexander, AKBAR, Mahesa, GUNAWAN, Leonardo, AULIA, Darryl Khalid, AGUNG, Rizqy, RAWIKARA, Seno Sahisnu, SASONGKO, Rianto Adhy and WIDAGDO, Djarot (2023). Evaluation of Piezoelectric-based Composite for Actuator Application via FEM with Thermal Analogy. *European Journal of Computational Mechanics*.

Copyright and re-use policy

See <http://shura.shu.ac.uk/information.html>

Evaluation of Piezoelectric-based Composite for Actuator Application via FEM with Thermal Analogy

Alexander Kevin^{1,*}, Mahesa Akbar^{1,2}, Leonardo Gunawan¹,
Darryl Khalid Aulia¹, Rizqy Agung¹, Seno Sahisnu Rawikara¹,
Rianto Adhy Sasongko¹ and Djarot Widagdo^{1,2}

¹*Faculty of Mechanical and Aerospace Engineering, Institut Teknologi Bandung, Jalan Ganesa No. 10, Bandung 40132, Indonesia*

²*Centre for Defence and Security Technology, Institut Teknologi Bandung, Jalan Ganesa No. 10, Bandung 40132, Indonesia*

E-mail: alexanderkevin0001@gmail.com

**Corresponding Author*

Received 14 April 2023; Accepted 05 September 2023;
Publication 29 December 2023

Abstract

In the present work, a new study on the piezoelectric-based structure by means of Finite Element Method (FEM) is conducted. Currently, the piezoelectric model in the FEM-based commercial software is only applicable via 2D plane stress and 3D solid elements. However, piezoelectric structures are usually manufactured as thin-walled structures, i.e., plates and disks. Therefore, it is more convenient to model a piezoelectric-based structure with 2D shell elements. In this study, FEM with a thermal analogy approach is implemented. Thermal coupling characteristics are utilised as the equivalent of electromechanical properties. Thermal analysis is much more established in FEM-based software; thus, applications with various types of elements are enabled. Therefore, the evaluation of piezoelectric structure via shell

European Journal of Computational Mechanics, Vol. 32_5, 495–518.

doi: 10.13052/ejcm2642-2085.3253

© 2023 River Publishers

element with a thermal analogy approach could be performed. Static and dynamic analyses are conducted with experimental and numerical validations. As depicted in some details in this paper, the shell model with thermal analogy shows an excellent agreement with the 3D solid piezoelectric elements with insignificant variances, less than 0.3%.

Keywords: Piezoelectric, finite element method (FEM), thermal analogy, actuator.

1 Introduction

Piezoelectric materials have become popular over the last three decades due to their electromechanical properties, i.e., actuating and sensing capabilities; thus, enabling versatile applications [1]. Growing applications of piezoelectric material are justified by their beneficial aspects, such as compact and space-saving constructions, high actuating precision, extremely short response times, absence of friction, vacuum and cleanroom capability, and the possibility of operation at cryogenic temperatures [2]. Innovative piezoelectric-based structure applications could be found in the fields of vibration control [3–5], structural health monitoring [6–9], and energy harvesting [10, 11].

As an actuator, piezoelectric materials allow the utilisation of an electrical load excitation to counteract mechanical responses induced by disturbances [2, 5]. In aerospace applications, piezoelectric-based structures are considered one of the alternatives for active vibration control [3, 4, 12].

The application in structural health monitoring uses the combination of piezoelectric-based sensors and actuators [8]. Damage detection could be enabled using the ability of piezoelectric material to generate and receive the strain waves propagated in a structure [7]. Furthermore, the electromechanical piezoelectric coupling effect is used to harvest the energy from mechanical vibration [10, 13]. Hence, recent studies seek much further development concerning self-sustained actuators and sensors, i.e., for aircraft vibration control and dynamic instability suppression [14].

Piezoelectric-based structures are usually arranged in a laminated composite-like manner, involving one or more piezoelectric layers that are stacked with a substructure material, i.e., isotropic material. Hence, there are also some focuses on the development of piezoelectric-based composites. One of the topics concerns the functionally graded material, or in this case functionally graded piezoelectric materials (FGPMs) [15, 16]. An FGPM

possesses variation of the mechanical and electrical properties in a spatial, i.e., thickness direction [15].

Numerous works have been conducted concerning FGPMs variations, i.e., for sandwich microplates [17, 18] and annular/circular sandwich microplates [19, 20]; exposure to various environments, including thermal [21, 22], magnetic [23], electromagnetic [24], thermal and magnetic field [25], hygrothermal [18], and hygromagneto-electro-thermal environments [26]. The state-of-the-art in this field discusses FGPMs as energy harvesting structures [27, 28].

In terms of computational methods, Finite Element Method (FEM) has been an established approach for structural analysis, including for composite structures. Shell and plate theories have been well developed for FEM with continuous improvement [29–31]. One of the earliest developments of piezoelectric structure using FEM was discussed by Tzou and Tseng [32].

The model by Tzou and Tseng [32] incorporates electrical potentials as additional degrees of freedom (DOFs) within a solid thin element. Furthermore, a model for laminated composites was proposed by Hwang and Park [33], employing bending plate elements. Both models described in [32] and [33] are applicable for evaluating piezoelectric-based sensors or actuators. Implementation of plate and shell theories for advanced piezoelectric composite has also been proposed in various studies, from the classical plate theory to a higher-order shear deformation theory [34], as well as for static and dynamic analyses [35, 36]. Moreover, new piezoelectric finite element concepts for energy harvesting have also been discussed in a few articles [37, 38].

Despite growing attention and expanding studies over the last decades, in FEM-based software, the options for piezoelectric-based elements are still limited. Currently, only 2D plane stress and 3D solid elements are available in commercial software [39]. In addition, most of the developments in piezoelectric elements requires extensive computational programming [40]. Therefore, the present work focuses on the utilisation of commercial software as much as possible to evaluate the piezoelectric-based structure.

The drawback of piezoelectric elements in commercial software comes from the implementation of 3D elements. Commonly, piezoelectric structures are manufactured in patches of thin-walled plates. Thus, a piezoelectric model via 3D elements will exhibit some shortfalls, i.e., very dense meshing configuration and over-stiffness in bending [40]. Moreover, the model with very thin elements requires special treatment to avoid issues such as shear and membrane locking [29]. From the previous studies, some alternative

techniques have been proposed to model piezoelectric structures in commercial software, i.e., equivalent circuits, spring models, and thermal analogy approach [39, 41].

In the present work, the so-called thermal analogy approach is implemented as an alternative to piezoelectric modelling. The choice of the thermal analogy method is due to its better compatibility with the thermal load module in FEM-based software. Early developments of the thermal analogy approach using FEM are discussed in [42–44]. The thermal load module is accessible and integrated into every commercial FEM-based software, and it can also be combined with other modules, such as the stress analysis module. In the most recent study, the thermal analogy approach was utilised to evaluate energy harvesting cases in combination with aeroelastic loads [40].

In this study, a new investigation by means of FEM with a thermal analogy approach is conducted with also experimental and numerical validations. One of the main focuses is the modelling of thin-walled piezoelectric patches via shell elements in commercial software. Static and dynamic analyses are done in this work. Moreover, the dynamic characteristics of the structure are compared to experimental results. For the first time, comparisons between 3D electromechanically coupled piezoelectric elements and shell elements with the thermal analogy method from commercial software are depicted. Some details on the results are discussed in the following sections.

2 Piezoelectric Constitutive Equations

Piezoelectric materials exhibit electromechanical coupling properties which defined as a cross-coupling between elasticity variables (stress and strain) and dielectric variables (electric field). Based on the IEEE Standard on Piezoelectricity [45], the electromechanical constitutive can be expressed:

$$\{T\} = [c^E]\{S\} - [e]^T\{E\} \quad (1)$$

$$\{D\} = [e]\{S\} + [\epsilon^S]\{E\} \quad (2)$$

where $\{T\}$ is the 6×1 stress vector, $[c^E]$ is the 6×6 elastic stiffness matrix under constant electric field conditions, $\{S\}$ is the 6×1 strain vector, $[e]$ is the 3×6 matrix of piezoelectric coupling coefficients that denote the coupling between the mechanical and electrical domains, $\{E\}$ is the 3×1 electric field vector, $\{D\}$ is the 3×1 electrical displacement vector, and $[\epsilon^S]$ is the 3×3 matrix of permittivity or free-body dielectric coefficient matrix under

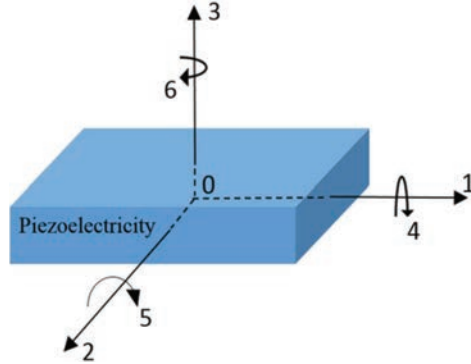


Figure 1 Tensor directions for defining constitutive equations [46].

constant strain conditions [40]. The tensor directions of the piezoelectric effect are illustrated in Figure 1.

The matrices s^E , d and ε^S depend on the symmetry centre of the anisotropic material used for the piezoelectric structure [2]. Furthermore, the type of piezoelectric material and its treatment determine the non-zero components of these matrices [45, 47]. Conventionally, the ferroelectric ceramics commonly employed by piezoelectric material manufacturers are polarized in the direction 3 and exhibit symmetry in their hexagonal crystallographic structure. As a result, the constitutive equations become [43]:

$$\begin{aligned}
 \begin{Bmatrix} T_1 \\ T_2 \\ T_3 \\ T_4 \\ T_5 \\ T_6 \end{Bmatrix} &= \begin{bmatrix} c_{11}^E & c_{12}^E & c_{13}^E & 0 & 0 & 0 \\ c_{21}^E & c_{11}^E & c_{13}^E & 0 & 0 & 0 \\ c_{13}^E & c_{13}^E & c_{33}^E & 0 & 0 & 0 \\ 0 & 0 & 0 & c_{44}^E & 0 & 0 \\ 0 & 0 & 0 & 0 & c_{44}^E & 0 \\ 0 & 0 & 0 & 0 & 0 & \frac{1}{2}(c_{11}^E - c_{12}^E) \end{bmatrix} \begin{Bmatrix} S_1 \\ S_2 \\ S_3 \\ S_4 \\ S_5 \\ S_6 \end{Bmatrix} \\
 &- \begin{bmatrix} 0 & 0 & e_{31} \\ 0 & 0 & e_{31} \\ 0 & 0 & e_{33} \\ 0 & e_{15} & 0 \\ e_{15} & 0 & 0 \\ 0 & 0 & 0 \end{bmatrix} \begin{Bmatrix} E_1 \\ E_2 \\ E_3 \end{Bmatrix} \quad (3)
 \end{aligned}$$

$$\begin{aligned}
\begin{Bmatrix} D_1 \\ D_2 \\ D_3 \end{Bmatrix} &= \begin{bmatrix} 0 & 0 & 0 & 0 & e_{15} & 0 \\ 0 & 0 & 0 & e_{15} & 0 & 0 \\ e_{31} & e_{31} & e_{33} & 0 & 0 & 0 \end{bmatrix} \begin{Bmatrix} S_1 \\ S_2 \\ S_3 \\ S_4 \\ S_5 \\ S_6 \end{Bmatrix} \\
&+ \begin{bmatrix} \epsilon_{11}^S & 0 & 0 \\ 0 & \epsilon_{11}^S & 0 \\ 0 & 0 & \epsilon_{33}^S \end{bmatrix} \begin{Bmatrix} E_1 \\ E_2 \\ E_3 \end{Bmatrix} \quad (4)
\end{aligned}$$

Piezoceramic manufacturers provide only the strain-charge form of the piezoelectric coupling coefficients $[d]$. The relationship between $[e]$ and $[d]$ is given as [43]:

$$[e] = [d][c^E] \quad (5)$$

3 Piezoelectric – Thermal Analogy

Direct numerical simulation of piezoelectric elements is not commonly available in commercial FEM-based software. Several commercial FEM-based software that include a built-in piezoelectric module are limited to 2D plane stress and 3D solid elements. However, piezoelectric structures are usually found in thin-walled structures. Consequently, piezoelectric modelling using 3D piezoelectric elements requires an exceedingly fine mesh, leading to high computational costs. Additionally, piezoelectric-based structural applications can induce bending and torsional deformations; thus, plane stress elements are not suitable.

The thermal analogy models the piezoelectric material based on the analogy between thermal strains and piezoelectric strains. Piezoelectric materials expand when electrical charges are applied to them. Similarly, materials also expand when subjected to a temperature difference. This thermal concept has been more established in FEM-based software than the piezoelectric concept. The generalized Hooke's law considering the thermal effect can be written as [43]:

$$\{T\} = [c^E]\{S\} - [c^E]\{\alpha\}\Delta\Theta \quad (6)$$

where $\{\alpha\}$ represents the 6×1 thermal expansion coefficient vector and $\Delta\Theta = \Theta - \Theta_0$ represents the temperature difference with respect to a reference temperature Θ_0 . Equation (6) illustrates the relationship between stress

and strain arising from mechanical loads (the first term on the right-hand side) and thermal loads (the second term on the right-hand side).

The expression in Equation (6) shares similarities with that of Equation (1). By comparing both equations, it becomes evident that the relationship between piezoelectric strains and thermal strains is:

$$\begin{aligned}
 [c^E]\{S\} - [e]^T\{E\} &= [c^E]\{S\} - [c^E]\{\alpha\}\Delta\Theta \\
 [e]^T\{E\} &= [c^E][d]^T\{E\} = [c^E]\{\alpha\}\Delta\Theta \\
 [d]^T\{E\} &= \{\alpha\}\Delta\Theta
 \end{aligned}
 \tag{7}$$

In matrix form, Equation (7) can be written as:

$$\begin{bmatrix} 0 & 0 & d_{31} \\ 0 & 0 & d_{31} \\ 0 & 0 & d_{33} \\ 0 & d_{15} & 0 \\ d_{15} & 0 & 0 \\ 0 & 0 & 0 \end{bmatrix} \begin{Bmatrix} \frac{\Delta\varphi_1}{t} \\ \frac{\Delta\varphi_2}{t} \\ \frac{\Delta\varphi_3}{t} \end{Bmatrix} = \begin{Bmatrix} \alpha_1 \\ \alpha_2 \\ \alpha_3 \\ \alpha_4 \\ \alpha_5 \\ \alpha_6 \end{Bmatrix} \Delta\Theta
 \tag{8}$$

where $\Delta\varphi$ represents the voltage difference and t is the thickness of the piezoceramic actuator. Equation (8) implies that the voltage actuation of piezoelectric materials can be simulated using conventional elastic elements with thermal actuation.

4 Piezoelectric Actuator Model

In the present work, two analyses were conducted by using Abaqus. First, the computational model using 3D solid piezoelectric elements was evaluated. Next, the piezoelectric structure was modelled using 2D shell finite elements with the thermal analogy. Both models – the 2D shell thermal analogy model and the 3D solid piezoelectric model – were investigated for their actuating mechanisms, and the results were then compared.

A piezoelectric-based composite known as a Macro Fiber Composite™ (MFC) [48] was used as the actuator. MFC structures have been utilised for various studies in structural vibration control [50, 51]. A unimorph plate structure with a layer of host structure and a layer of piezoelectric patch was studied. The dimensions of the unimorph plate are 340 mm × 38 mm × 1 mm for the host structure (aluminium) and 28 mm × 14 mm × 0.3 mm

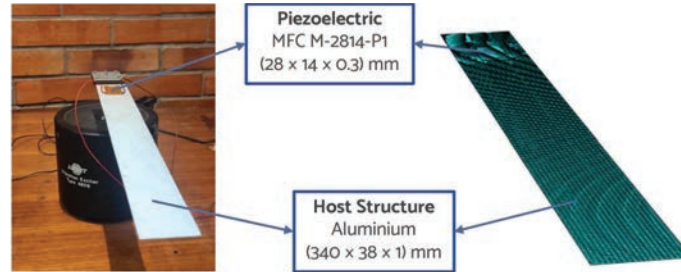


Figure 2 The FE model of the unimorph plate (right) compared with the experimental model (left).

Table 1 The material properties of aluminium and piezoelectric [48, 49]

Material Property	Symbol (Unit)	Aluminium	Piezoelectric
Density	ρ (kg/m ³)	2604	5440
Young's modulus	E (GPa)	51.44	30.34
Poisson's ratio	ν (–)	0.33	0.31
Piezoelectric coefficient	d_{31} (pC/N)	–	–170
	d_{33} (pC/N)	–	400
Dielectric	$\epsilon_{33}^T/\epsilon_0$ (–)	–	1593

for the MFC actuator, as depicted in Figure 2 (right). In the current study, the dimensions of the unimorph plate were chosen to represent a typical microsatellite panel. In such cases, the first bending frequency is usually below 10 Hz, and the second frequency is in the order of tens Hz [52, 53]. The properties of both aluminium and the piezoelectric materials are listed in Table 1.

In this study, an experimental model was also created to assess the dynamic characteristics of the unimorph plate. An illustration of the unimorph plate used in the experiment is displayed in Figure 2 (left). A preliminary experimental test yielded a structural damping value of approximately 1.6% for the unimorph plate. This damping value was subsequently incorporated into the finite element model to complete the material properties.

5 Computational Analysis

5.1 Unimorph Dynamic Characteristics

This section presents the structural dynamic analysis of the unimorph plate with the piezoelectric used as a sensor. In the FEM model, the host structure

Table 2 The natural frequencies of the first three bending modes

Mode Shape	Natural Frequency (Hz)			Variance	
	Experiment	Piezoelectric Element	Thermal Analogy	Piezoelectric Element	Thermal Analogy
1st bending	6.40	6.45	6.43	0.83%	0.45%
2nd bending	39.00	39.46	39.43	1.18%	1.09%
3rd bending	114.50	109.54	109.52	4.33%	4.35%

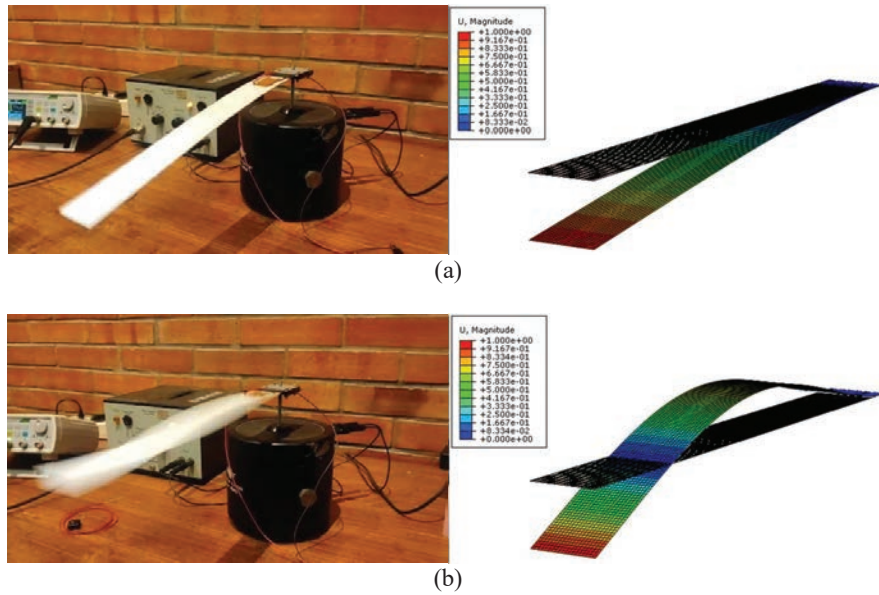


Figure 3 Comparison of mode shapes between experiment and numerical results for (a) first bending and (b) second bending.

was represented by using four-noded linear quadrilateral shell elements with reduced integration (S4R element type in Abaqus). The MFC was modelled using two different approaches: shell elements for the thermal analogy approach and solid electromechanical piezoelectric elements. In this case, the solid twenty-noded hexahedron piezoelectric elements with reduced integration (C3D20RE element type in Abaqus) were chosen.

The natural frequencies and mode shapes of the unimorph plate are displayed in Table 2 and Figure 3. After that, the dynamic analysis was conducted in the frequency domain by applying base excitation at the root of the specimen. The frequency response functions obtained from both numerical and experimental methods are illustrated in Figure 4. The results obtained

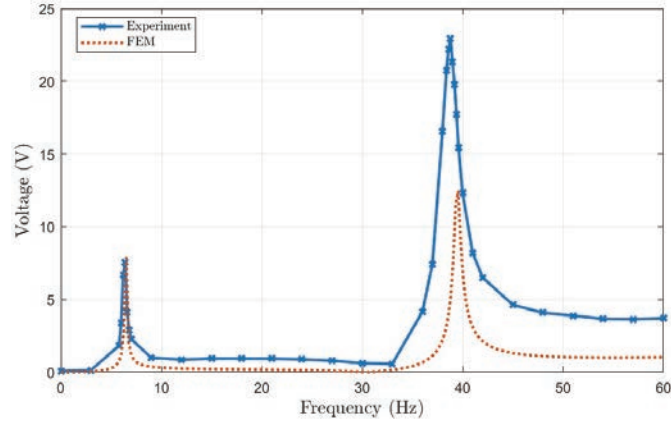


Figure 4 The frequency response of the unimorph plate.

from modal analysis and frequency response analysis exhibit significant agreement in terms of natural frequencies. As a result, the FE model can be confidently employed for subsequent analyses.

5.2 Piezoelectric Actuator Analysis

This section presents the numerical results of the unimorph plate with the piezoelectric used as an actuator. The two numerical models – finite elements with thermal analogy and 3D piezoelectric finite elements – were evaluated and compared.

Utilising the thermal analogy, the piezoelectric structure can be modelled using shell elements. Similar to the model employing 3D piezoelectric elements, the aluminium beam was represented by linear quadrilateral shell elements. However, a key distinction lied in the region containing the piezoelectric material. In this area, laminated composite shell elements comprising both aluminium and piezoelectric layers were employed. According to Equation (8), the thermal expansion coefficients of the piezoelectric layer were $\alpha_1 = \alpha_2 = -1.7 \times 10^{-10} \text{ }^\circ\text{C}$ and $\alpha_3 = 4 \times 10^{-10} \text{ }^\circ\text{C}$.

A static analysis was conducted by applying a constant voltage to the piezoelectric material. The analysis utilised voltages of 50 V, 75 V, 100 V, 125 V, and 150 V. Consequently, the corresponding temperature differences, calculated using Equation (8), amounted to 167000°C, 250000°C, 333000°C, 417000°C, and 500000°C, respectively. The host structure was clamped at the root, and the resulting vertical displacement of the beam was evaluated. The static analysis results are depicted in Figures 5 and 6.

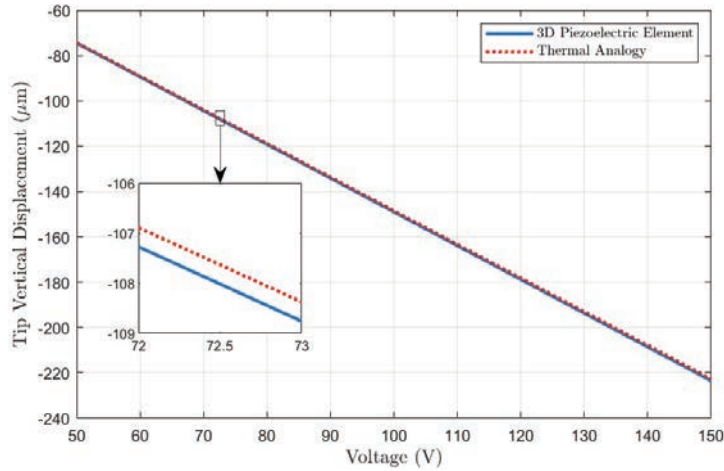


Figure 5 The relation between tip vertical displacement and voltage based on 3D piezoelectric element and thermal analogy.

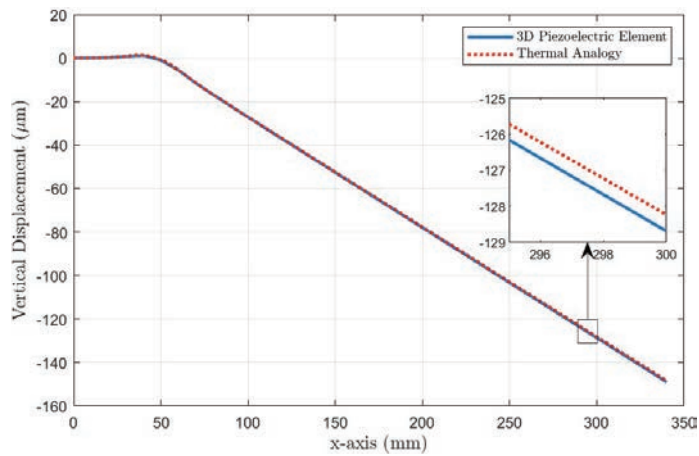


Figure 6 The vertical displacement along the length of the beam when the piezoelectric is subjected to 100 V based on 3D piezoelectric elements and thermal analogy.

Figure 5 presents the correlation between the vertical tip displacement of the host structure and varying voltage inputs. As evident from Figure 5, a linear relationship exists between the vertical displacement of the host structure and the voltage input. Notably, a higher voltage input corresponds to a greater vertical displacement of the host structure. Moving to Figure 6,

the vertical displacement of the host structure is shown along the length of the beam when the piezoelectric is subjected to a 100 V input. In Figure 6, a peak appears at the x-axis value of 40 mm. This peak is a consequence of the presence of the piezoelectric patch in that particular region. The piezoelectric material imparts bending to the host structure. However, due to the clamped boundary condition at the root of the beam, the piezoelectric attempts to induce bending results in a positive vertical displacement instead. Analysing the static analysis results, the difference between the results obtained through the thermal analogy and those using 3D piezoelectric elements is approximately 0.3%. This close correspondence demonstrates a strong agreement between the outcomes of both methods. Consequently, the thermal analogy method effectively predicts vertical displacement in the context of static analysis.

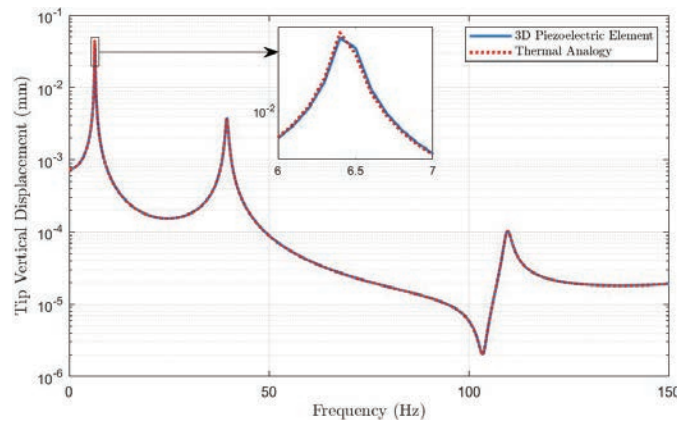


Figure 7 The frequency response function of the model based on 3D piezoelectric elements and thermal analogy.

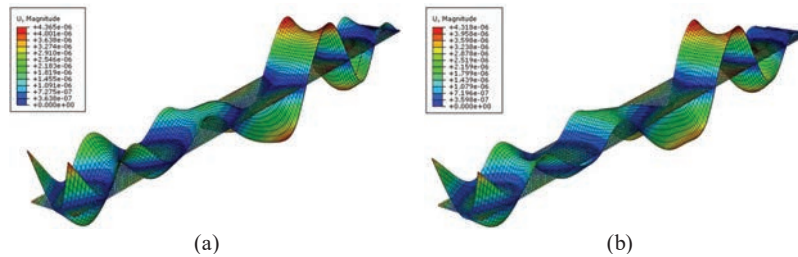


Figure 8 The comparison of displacement contour from FEM at $t = 5$ ms based on (a) 3D solid piezoelectric elements and (b) thermal analogy with shell elements.

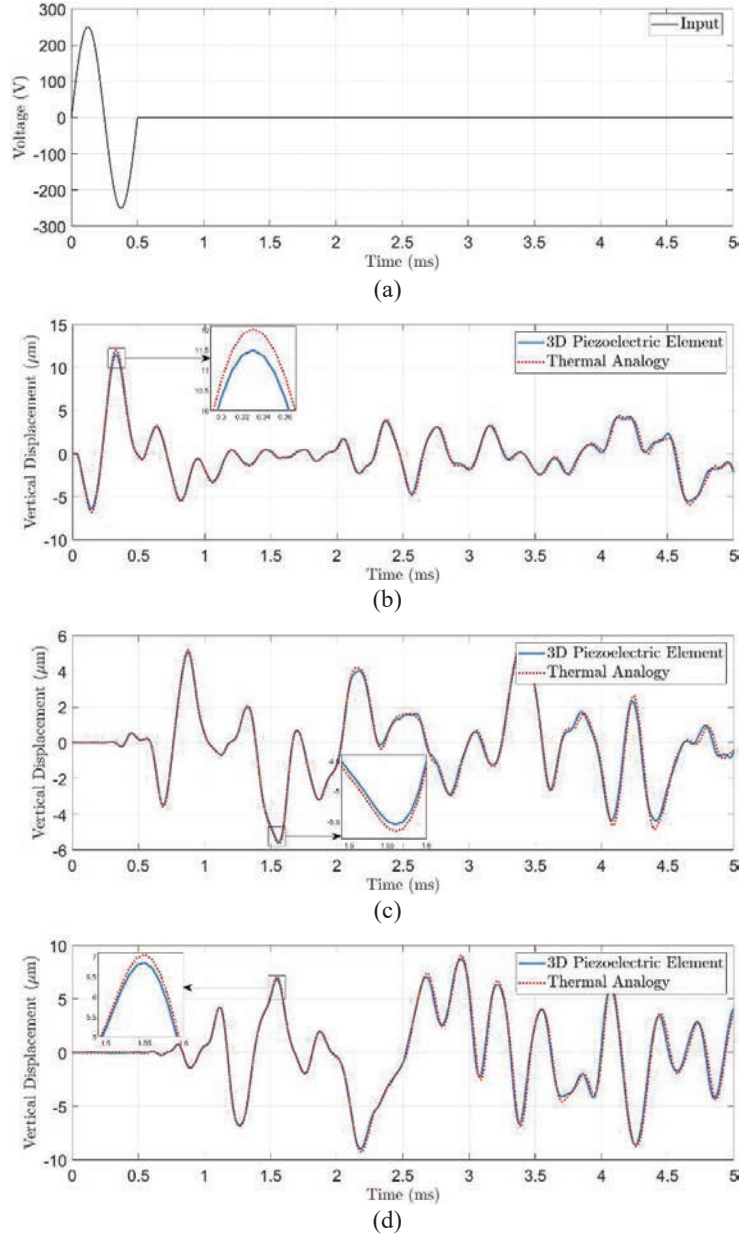


Figure 9 (a) The voltage input used for the time response analysis; the result of time response analysis of the model at (b) 45 mm from the clamp, (c) 200.5 mm from the clamp, and (d) 340 mm from the clamp based on 3D piezoelectric elements and thermal analogy.

Additionally, a dynamic analysis was conducted using both frequency response analysis and time response analysis. For frequency response analysis, a sinusoidal voltage was applied to the piezoelectric material with an amplitude of $\Delta\varphi_3 = 0.5$ V, i.e., $\Delta\Theta = 1667$ °C for the thermal analogy model. This analysis aimed to observe the effect of frequency on the tip's vertical displacement and to compare it with the results obtained from the finite element approach using three-dimensional piezoelectric elements. The results of the frequency response analysis are presented in Figure 7.

In the time response analysis, a single sinusoidal pulse with an amplitude of 250 V, i.e., $\Delta\Theta = 833,333$ °C for the thermal analogy, and a period of 500 μ s was applied to the piezoelectric surface. The analysis focused on measuring the vertical displacement at three specific points along the length of the beam's edge: 45 mm, 200.5 mm, and 340 mm from the clamp. The results from the thermal analogy method were compared with those of the finite element analysis based on the three-dimensional piezoelectric elements. The results of the time response analysis are illustrated in Figures 8 and 9.

Based on the results from the frequency response analysis in Figure 7 and the time response analysis in Figure 9, a notable alignment is observed between the 2D shell model utilising thermal analogy and the model employing 3D piezoelectric elements. The discrepancy between both modelling approaches is approximately 0.3% in the frequency response analysis. Similarly, in the time response analysis, the behaviour of the unimorph plate closely resembles that of both the thermal analogy and the 3D piezoelectric element models. Consequently, the thermal analogy method effectively predicts the dynamic response of the piezoelectric material.

6 Conclusion

In this study, an evaluation of a piezoelectric-based composite structure has been carried out employing FEM with a thermal analogy approach. By employing the thermal analogy, the piezoelectric structure has been effectively modelled and evaluated using 2D shell elements in FEM-based software. This shell model has proven a suitable representation of a piezoelectric patch as a thin-walled structure. The comparison between the model with the thermal analogy approach and the 3D electromechanical piezoelectric elements has demonstrated excellent agreement. In addition, the dynamic characteristics of the structure have been successfully validated against experimental results.

The results obtained through the thermal analogy approach have shown insignificant discrepancies (less than 0.3%) in both static and dynamic responses when compared with the 3D model utilising electromechanical piezoelectric elements. Therefore, based on the current results, the thermal analogy approach holds promise as an alternative method for evaluating piezoelectric-based structures, particularly in representing them as thin-walled structures.

References

- [1] A. Aabid, B. Parveez, M. A. Raheman, Y. E. Ibrahim, A. Anjum, M. Hrairi, N. Parveen and J. M. Zayan, "A review of piezoelectric material-based structural control and health monitoring techniques for engineering structures: Challenges and opportunities," *Actuators*, no. 10, pp. 1–26, 2021.
- [2] R. G. Ballas, *Piezoelectric Multilayer Beam Bending Actuators*, H. Fujita and D. Liepmann, Eds., New York: Springer-Verlag Berlin Heidelberg, 2007.
- [3] I. M. d. Fonseca, D. A. Rade, L. C. Goes and T. d. P. Sales, "Attitude and vibration control of a satellite containing flexible solar arrays by using reaction wheels, and piezoelectric transducers as sensors and actuators," *Acta Astronautica*, vol. 139, pp. 357–366, 1 July 2017.
- [4] Q. Yuan, Y. Liu and N. Qi, "Active vibration suppression for maneuvering spacecraft with high flexible appendages," *Acta Astronautica*, vol. 139, pp. 512–520, 1 July 2017.
- [5] K. Uchino, "Piezoelectric actuators 2004 – materials, design, drive/control, modeling and applications," in *Actuator 2004, 9th International Conference on New Actuators*, Bremen, 2004.
- [6] S. Petit, "Impact and compression after impact experimental study of a composite laminate with a cork thermal shield," *Composites Science and Technology*, vol. 67, no. 15–16, pp. 3286–3299, 2007.
- [7] Z. Su and L. Ye, *Identification of Damage Using Lamb Waves – From Fundamentals to Applications*, Heidelberg: Springer, 2008.
- [8] Z. Sharif-Khodaei, M. Ghajari and M. H. Aliabadi, "Determination of impact location on composite stiffened panels," *Smart Materials and Structures*, vol. 21, no. 10, p. 105026, 2012.
- [9] L. Gunawan, M. H. Farrasamulya, A. Kuswoyo and T. Dirgantara, "Development of laboratory-scale Lamb wave-based health monitoring

- system for laminated composites,” *Journal of Engineering and Technological Sciences*, vol. 53, no. 4, pp. 675–694, 2021.
- [10] S. R. Anton and D. J. Inman, “Vibration energy harvesting for unmanned aerial vehicles,” in *Proceedings of SPIE*, 2008.
- [11] M. Akbar and J. Curiel-Sosa, “Piezoelectric energy harvester composite under dynamic bending with implementation to aircraft wingbox structure,” *Composite Structures*, vol. 153, 2016.
- [12] C. K. Susheel, R. Kumar, V. S. Chauhan and R. Vaish, “Shape control of spacecraft antenna reflector using lead-free piezoelectric actuators,” *European Journal of Computational Mechanics*, vol. 23, no. 5–6, pp. 199–216, 2014.
- [13] M. Akbar and J. L. Curiel-Sosa, “Implementation of multiphase piezoelectric composites energy harvester on aircraft wingbox structure with fuel saving evaluation,” *Composite Structures*, vol. 202, pp. 1000–1020, 2018.
- [14] N. Tsushima and W. Su, “A study on adaptive vibration control and energy conversion of highly flexible multifunctional wings,” *Aerospace Science and Technology*, vol. 79, pp. 297–309, 2018.
- [15] C. Wu, M. Kahn and W. Moy, “Piezoelectric ceramics with functional gradients: a new application in material design,” *Journal of the American Ceramic Society*, vol. 79, no. 3, pp. 809–812, 2005.
- [16] X. Zhu and Z. Meng, “Operational principle, fabrication and displacement characteristics of a functionally gradient piezoelectric ceramic actuator,” *Sensors and Actuators A: Physical*, vol. 48, no. 3, pp. 169–176, 1995.
- [17] E. Arshid, S. Amir and A. Loghman, “On the vibrations of FG GNPs-RPN annular plates with piezoelectric/metallic coatings on Kerr elastic substrate considering size dependency and surface stress effects,” *Acta Mechanica*, vol. 234, no. 9, pp. 1–42, 2023.
- [18] E. Arshid, M. Khorasani, Z. Soleimani-Javid, S. Amir and A. Tounsi, “Porosity-dependent vibration analysis of FG microplates embedded by polymeric nanocomposite patches considering hygrothermal effect via an innovative plate theory,” *Engineering with Computers*, vol. 38, no. 5, pp. 4051–4072, 2022.
- [19] E. Arshid, S. Amir and A. Loghman, “Bending and buckling behaviors of heterogeneous temperature-dependent micro annular/circular porous sandwich plates integrated by FGPEM nano-Composite layers,” *Journal of Sandwich Structures and Materials*, vol. 0, no. 0, pp. 1–42, 2020.

- [20] E. Arshid, S. Amir and A. Loghman, “Thermoelastic vibration characteristics of asymmetric annular porous reinforced with nano-fillers microplates embedded in an elastic medium: CNTs Vs. GNPs,” *Archives of Civil and Mechanical Engineering*, vol. 23, no. 100, pp. 1–28, 2023.
- [21] E. Arshid, S. Amir and A. Loghman, “Thermal buckling analysis of FG graphene nanoplatelets reinforced porous nanocomposite MCST-based annular/circular microplates,” *Aerospace Science and Technology*, vol. 111, p. 106561, 2021.
- [22] Z. Soleimani-Javid, E. Arshid, S. Amir and M. Bodaghi, “On the higher-order thermal vibrations of FG saturated porous cylindrical micro-shells integrated with nanocomposite skins in viscoelastic medium,” *Defence Technology*, vol. 18, pp. 1416–1434, 2022.
- [23] S. Amir, E. Arshid, Z. K. Maraghi, A. Loghman and A. G. Arani, “Vibration analysis of magnetorheological fluid circular sandwich plates with magnetostrictive facesheets exposed to monotonic magnetic field located on visco-Pasternak substrate,” *Journal of Vibration and Control*, vol. 0, no. 0, pp. 1–15, 2020.
- [24] M. Khorasani, Z. Soleimani-Javid, E. Arshid, S. Amir and Ö. Civalek, “Vibration analysis of graphene nanoplatelets’ reinforced composite plates integrated by piezo-electromagnetic patches on the piezo-electromagnetic media,” *Waves in Random and Complex Media*, pp. 1–31, 2021.
- [25] E. Arshid, H. Arshid, S. Amir and S. B. Mousavi, “Free vibration and buckling analyses of FG porous sandwich curved microbeams in thermal environment under magnetic field based on modified couple stress theory,” *Archives of Civil and Mechanical Engineering*, vol. 21, no. 6, pp. 1–23, 2021.
- [26] E. Arshid, Z. Soleimani-Javid, S. Amir and N. D. Duc, “Higher-order hygro-magneto-electro-thermomechanical analysis of FG-GNPs-reinforced composite cylindrical shells embedded in PEM layers,” *Aerospace Science and Technology*, vol. 126, p. 107573, 2022.
- [27] Y. Amini, H. Emdad and M. Farid, “Finite element modeling of functionally graded piezoelectric harvesters,” *Composite Structures*, vol. 129, 2015.
- [28] M. Heshmati and Y. Amini, “A comprehensive study on the functionally graded piezoelectric energy harvesting from vibrations of a graded beam under travelling multi-oscillators,” *Applied Mathematical Modelling*, vol. 66, pp. 344–361, 2019.

- [29] H. L. Ton-That, H. Nguyen-Van and T. Chau-Dinh, “Static and buckling analyses of stiffened plate/shell structures using the quadrilateral element SQ4C,” *Comptes Rendus Mecanique*, vol. 348, no. 4, pp. 285–305, 2020.
- [30] H. L. Ton-That, “Improvement on eight-node quadrilateral element (IQ8) using twice-interpolation strategy for linear elastic fracture mechanics,” *Engineering Solid Mechanics*, vol. 8, pp. 323–336, 2020.
- [31] H. L. Ton-That, “Plate structural analysis based on a double interpolation element with arbitrary meshing,” *Acta Mechanica et Automatica*, vol. 15, no. 2, pp. 91–99, 2021.
- [32] H. S. Tzou and C. I. Tseng, “Distributed piezoelectric sensor/actuator design for dynamic measurement/control of distributed parameter systems: A piezoelectric finite element approach,” *Journal of Sound and Vibration*, vol. 138, no. 1, pp. 17–34, 1990.
- [33] W.-S. Hwang and H. C. Park, “Finite element modeling of piezoelectric sensors and actuators,” *AIAA Journal*, vol. 31, no. 5, pp. 930–937, 1993.
- [34] E. Arshid, A. R. Khorshidvand and S. M. Khorsandijou, “The effect of porosity on free vibration of SPFG circular plates resting on visco-Pasternak elastic foundation based on CPT, FSDT and TSDT,” *Structural Engineering and Mechanics*, vol. 70, no. 1, pp. 97–112, 2019.
- [35] E. Arshid and A. R. Khorshidvand, “Free vibration analysis of saturated porous FG circular plates integrated with piezoelectric actuators via differential quadrature method,” *Thin-Walled Structures*, vol. 125, pp. 220–233, 2018.
- [36] E. Arshid, S. Amir and A. Loghman, “Static and dynamic analyses of FG-GNPs reinforced porous nanocomposite annular micro-plates based on MSGT,” *International Journal of Mechanical Sciences*, vol. 180, p. 105656, 2020.
- [37] M. Akbar and J. L. Curiel-Sosa, “Evaluation of piezoelectric energy harvester under dynamic bending by means of hybrid mathematical/isogeometric analysis,” *International Journal of Mechanics and Materials in Design*, vol. 14, pp. 647–667, 2018.
- [38] C. De Marqui Junior, A. Erturk and D. J. Inman, “An electromechanical finite element model for piezoelectric energy harvester plates,” *Journal of Sound and Vibration*, vol. 327, no. 1–2, pp. 9–25, 2009.
- [39] M. Staworko and T. Uhl, “Modeling and simulation of piezoelectric elements – comparison of available methods and tools,” *Mechanics*, vol. 27, no. 4, pp. 161–171, 2008.

- [40] M. Akbar and J. L. Curiel-Sosa, "An iterative finite element method for piezoelectric energy harvesting composite with implementation to lifting structures under gust load conditions," *Composite Structures*, vol. 219, pp. 97–110, 1 July 2019.
- [41] M. M. Chaabane, R. Plateaux, J. -Y. Choley, C. Karra, A. Riviere and M. Haddar, "New topological approach for the modelling of mecatronic systems: application for piezoelectric structures," *European Journal of Computational Mechanics*, vol. 22, no. 2–4, pp. 209–227, 2013.
- [42] B. D. Freed and V. Babuška, "Finite element modeling of composite piezoelectric structures with MSC/NASTRAN," in *Smart Structures and Materials 1997: Smart Structures and Integrated Systems*, San Diego, 1997.
- [43] F. Côté, P. Masson, N. Mrad and V. Cotoni, "Dynamic and static modelling of piezoelectric composite structures using a thermal analogy with MSC/NASTRAN," *Composite Structures*, vol. 65, pp. 471–484, 1 September 2004.
- [44] X.-J. Dong and G. Meng, "Dynamic analysis of structures with piezoelectric actuators based on thermal analogy method," *The International Journal of Advanced Manufacturing Technology*, vol. 27, pp. 841–844, 1 February 2006.
- [45] A. Meitzler, H. F. Tiersten, A. W. Warner, D. Belincourt, G. A. Couquin and F. S. Welsh III, "IEEE Standard on Piezoelectricity – Standards Committee of the IEEE Ultrasonics," *Ferroelectrics, and Frequency Control Society*, p. 66, 1987.
- [46] V. Nguyen, N. Wu and Q. Wang, "A review on energy harvesting from ocean waves by piezoelectric technology," *Journal of Modeling in Mechanics and Materials*, 2017.
- [47] R. Dahiya and M. Valle, *Robotic Tactile Sensing – Technologies and System*, Berlin: Springer Science + Business Media, 2011.
- [48] "Smart Material," [Online]. Available: <https://www.smart-material.com/>.
- [49] A. Deraemaeker, H. Nasser, A. Benjeddou and A. Preumont, "Mixing rules for the piezoelectric properties of Macro Fiber Composites," *Journal of Intelligent Material Systems and Structures*, vol. 20, pp. 1475–1482, 31 July 2009.
- [50] A. Kovalovs, B. Evgeny and S. Gluhihs, "Active control of structures using macro-fiber composite (MFC)," *Journal of Physics: Conference Series*, vol. 93, p. 012034, 20 December 2007.

- [51] J. Gawryluk, A. Mitura and A. Teter, “Dynamic control of kinematically excited laminated, thin-walled beam using macro fibre composite actuator,” *Composite Structures*, vol. 236, p. 111898, 1 March 2020.
- [52] G. Ma, M. Xu, J. Tian and X. Kan, “The vibration suppression of solar panel based on smart structure,” *The Aeronautical Journal*, vol. 125, no. 1283, pp. 1–12, 2020.
- [53] M. M. Ataei, H. Salarieh, H. N. Pishkenari and H. Jalili, “Boundary control design for vibration suppression and attitude control of flexible satellites with multi-section appendages,” *Acta Astronautica*, vol. 173, no. 15, 2020.

Biographies



Alexander Kevin received his master’s degree in aerospace engineering from Institut Teknologi Bandung (Indonesia) in 2023. He is currently working as a Research Assistant at the Lightweight Structure Research Group, Faculty of Mechanical and Aerospace Engineering, Institut Teknologi Bandung. His research interest is in the field of computer-aided engineering (CAE) related to solid mechanics and structural dynamics.



Mahesa Akbar received the philosophy of doctorate degree in Mechanical Engineering from The University of Sheffield in 2019. He is currently working as a Researcher at the Centre of Defence and Security Technology

and Lightweight Structure Research Group at Institut Teknologi Bandung. His expertise is in the field of computer-aided engineering (CAE) with interests in structural dynamics, fluid dynamics, aeroelasticity, fluid-structure interaction, energy harvesting and smart composites.



Leonardo Gunawan received the philosophy of doctorate degree from Delft University of Technology in 1988. He is a Professor in Structural Dynamics at the Faculty of Mechanical and Aerospace Engineering, Institut Teknologi Bandung. He has more than 20 years of experience in the fields of structural dynamics and aeroelasticity.



Darryl Khalid Aulia received his bachelor's degree in aerospace engineering from Institut Teknologi Bandung (Indonesia) in 2023. He is currently taking in Master of Engineering in Aerospace Science & Engineering at the University of Toronto. His research interest is in the field of aerospace material science.



Rizqy Agung received his master's degree in aerospace engineering from Institut Teknologi Bandung in 2023. He is currently working as an Engineer at Turkish Aerospace Indonesia. His expertise is in the field of structural dynamics and aeroelasticity.



Seno Sahisnu Rawikara received his master's degree in aerospace engineering from Institut Teknologi Bandung in 2015. Currently, he is a Lecturer/Assistant Professor at the aerospace department in Institut Teknologi Bandung while pursuing a PhD degree in Control Systems Research Group at the University of Exeter. His research interest is in the field of flight control design, especially in the application of fault-tolerant control systems in aerospace systems.



Rianto Adhy Sasongko received the philosophy of doctorate degree from Imperial College London in 2008. He is an Associate Professor at the Faculty

of Mechanical and Aerospace Engineering, Institut Teknologi Bandung. He is currently the Head of the Aerospace Engineering Undergraduate Study Programme. He has more than 15 years of experience in the fields of aircraft control and aeroelasticity.



Djarot Widagdo received the philosophy of doctorate degree from Queen Mary University in 2004. He is an Assistant Professor at the Faculty of Mechanical and Aerospace Engineering, Institut Teknologi Bandung. He is currently the Head of the Centre of Defence and Security Technology. He has more than 15 years of experience in the fields of solid mechanics and aircraft structural design.

